

## SUPPORTING INFORMATION (S.I.)

### **Bioactive Hydrogels based on Lysine Dendrigrfts as Crosslinkers: Tailoring Elastic Properties to Influence hMSC Osteogenic Differentiation**

Michele Valeo,<sup>a</sup> Sébastien Marie,<sup>b</sup> Murielle Rémy,<sup>a</sup> Tiphaine Menguy,<sup>b</sup> Cédric Le Coz,<sup>c</sup> Michael Molinari,<sup>a</sup> Cécile Feuillie,<sup>a</sup> Fabien Granier,<sup>b</sup> and Marie-Christine Durrieu\*<sup>a</sup>.

<sup>a</sup> Université de Bordeaux, CNRS, Bordeaux INP, CBMN, UMR 5248, Pessac.

<sup>b</sup> FGHI, Montarnaud.

<sup>c</sup> Université de Bordeaux, CNRS, Bordeaux INP, LCPO, ENSMAC, Pessac.

#### **Figures**

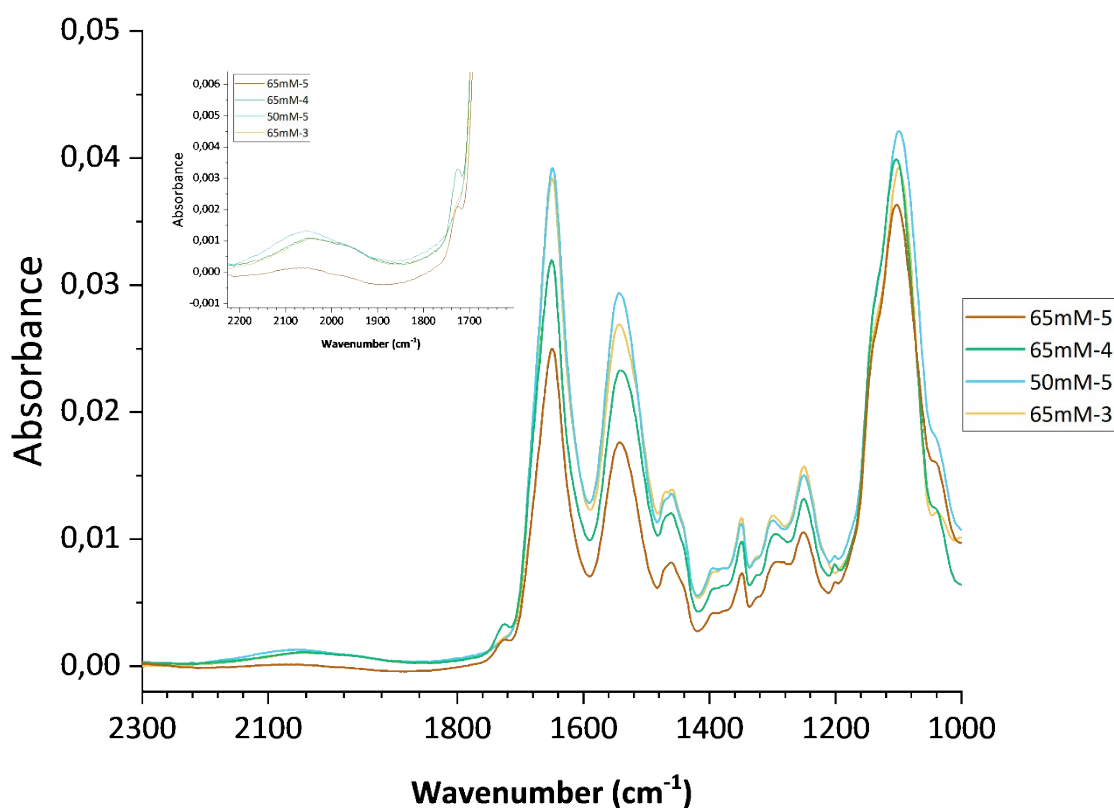


**Figure S1:** FT-ATR spectra of lyophilized DGL G5-PEG hydrogels before surface functionalization, showing the functional groups region (2300 – 1000  $\text{cm}^{-1}$ ). The central portion of the spectrum is occupied by the amide I and II bands at 1648  $\text{cm}^{-1}$  and 1560  $\text{cm}^{-1}$ , respectively. At the right end, the shouldered peak at 1100  $\text{cm}^{-1}$  is the C-O stretching of the dicarboxylic-PEG, not showing differences between the 50 and 65mM gels. Of note, a broad and weak signal is present at  $\approx 2100 \text{ cm}^{-1}$ , indicating carbodiimide traces. Interestingly, the small peak at 1730  $\text{cm}^{-1}$ , attributed to the stretching of uncrosslinked COOH groups in the PEG, indicates the quantitative reaction of the dicarboxylic acid-PEG chains with the terminal amines of DGL G5.

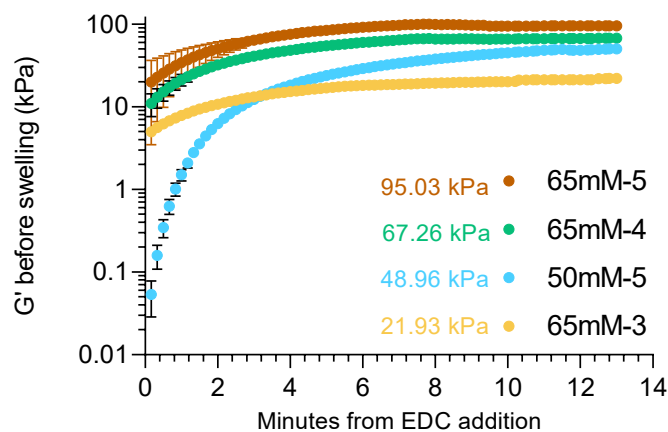


**Figure S2: Time sweeps of *in situ*-polymerized DGL G5-PEG hydrogels.** Hydrogels of the same dicarboxylic acid-PEG content (65mM-5) show symmetric curves, indicating similar crosslinking rates.

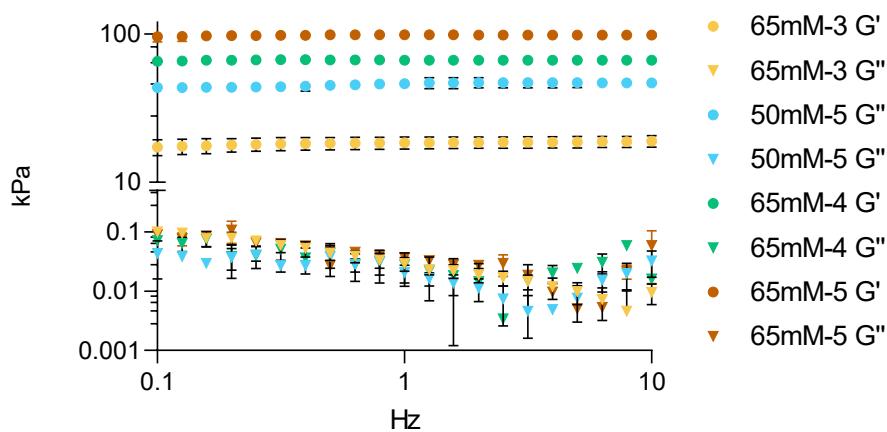


**Figure S3: frequency sweeps of selected DGL G5-PEG hydrogels before swelling (1% shear strain).** The storage modulus ( $G'$ ) is reported in circles and the loss modulus ( $G''$ ) in triangles. Storage modulus at 1Hz was  $18,45 \pm 1,72$  (65mM-3),  $46,33 \pm 3,28$  (50mM-5),  $66,73 \pm 0,898$  (65mM-4) and  $98,83 \pm 4,23$  (65mM-5).

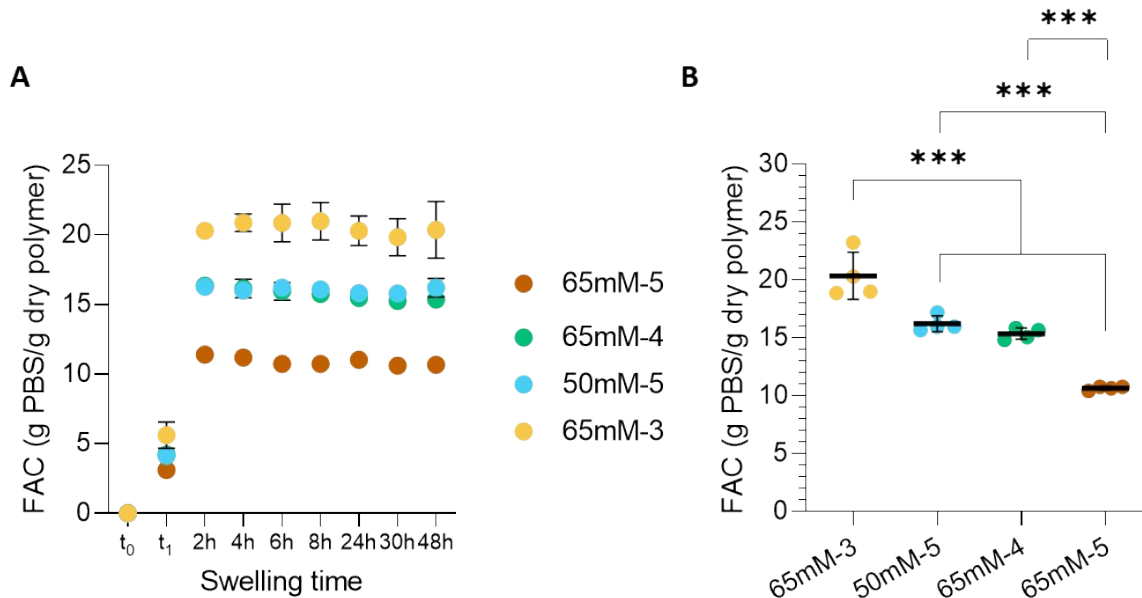


**Figure S4: swelling kinetics of selected DGL G5-PEG gels.** (A), fluid absorption capacity (FAC) expressed as fold increment of the dry hydrogel weight  $W_0$  (taken as the 0 in  $t_0$ ), in PBS at r.t. ( $t_1$  is the hydrogel weight after crosslinking and before swelling). Having polyelectrolyte character due to protonated amine groups at physiological pH, DGL G5-PEG hydrogels exhibited fast swelling at room temperature, reaching equilibrium in approximately 2h. (B), equilibrium fluid absorption capacity (FAC), indicating the g PBS absorbed by each g of dry polymer. At equilibrium, 65mM-3 gels absorbed approximately 20 times their initial dry weight ( $W_0$ ) in PBS, 50mM-5 and 65mM-4 gels 15 times, and 65mM-5 gels 10 times. ONE-WAY ANOVA (with Tuckey's correction for multiple comparisons) analysis, with  $P < 0.05$  (\*),  $P < 0.01$  (\*\*),  $P < 0.001$  (\*\*\*). Not significant =  $P > 0.05$ . All statistical tests are reported at the end of the Supplementary Information.

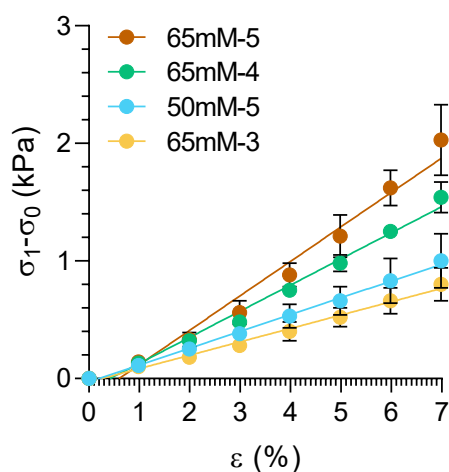


**Figure S5: stress-strain curves of non-functionalised, swollen DGL G5-PEG hydrogels.** Uniaxial strain was measured in non-confined compression up to 5% of the initial length.

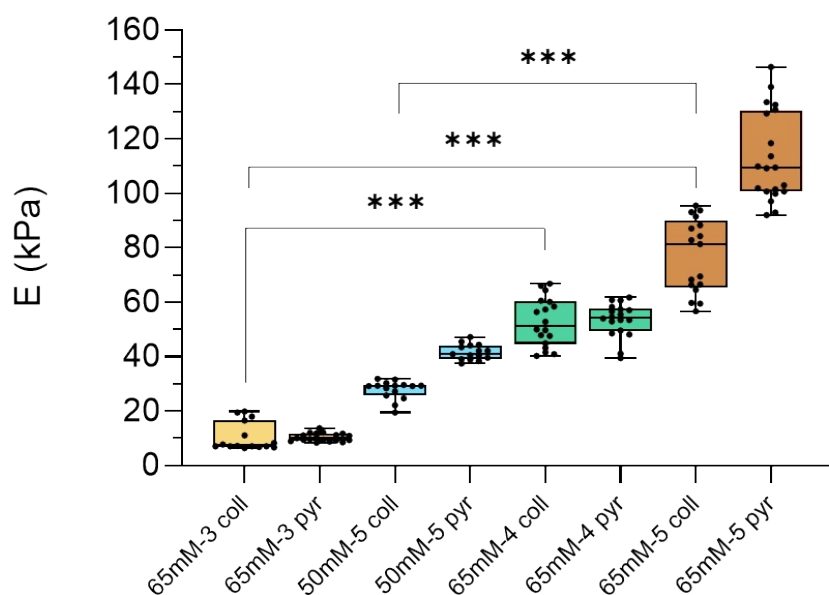


**Figure S6: paired comparison of surface E values obtained by AFM indentations with a colloidal (coll) or pyramidal (pyr) tip.** Each point represents the averaged E value over a squared array of  $400 \mu\text{m}^2$  ( $20 \times 20$ ). At least five different regions were analysed per gel. No statistical difference was found in paired E values obtained with the colloidal or pyramidal tip geometry. Group comparisons of data obtained with the colloidal tip showed statistical significance only among non-nearby groups. N (gels) = 3, non-parametric analysis (Kruskal-Wallis test) with  $P < 0.05$  (\*),  $P < 0.01$  (\*\*),  $P < 0.001$  (\*\*\*) . All statistical tests are reported at the end of the Supplementary Information.

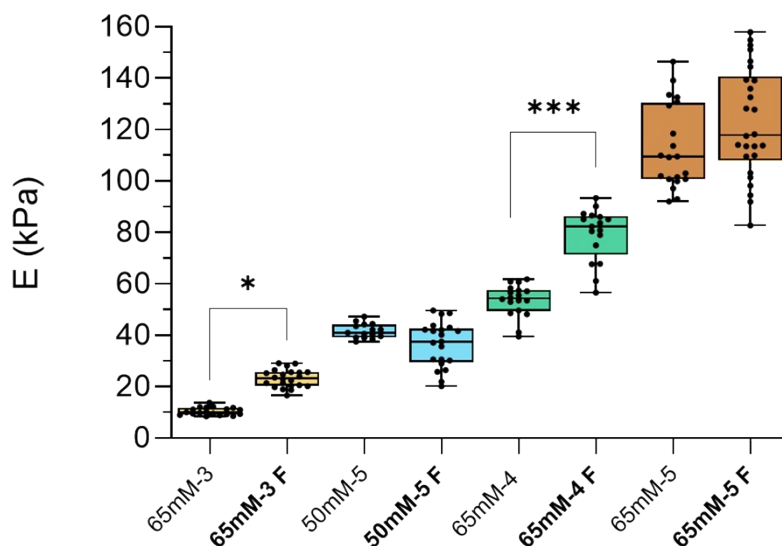


**Figure S7: paired comparison of surface E values measured with a pyramidal tip before and after (F) functionalisation with GRGDSPC and BMP-2 mimetic peptides.** Each point represents the averaged E value over a squared array of  $400 \mu\text{m}^2$  ( $20 \times 20$ ). At least five different regions were analysed per gel. N (gels) = 3, One-way ANOVA (Tukey's correction for multiple comparisons) with  $P < 0.05$  (\*),  $P < 0.01$  (\*\*),  $P < 0.001$  (\*\*\*) . Not significant =  $P > 0.05$ . All statistical tests are reported All statistical tests are reported at the end of the Supplementary Information.

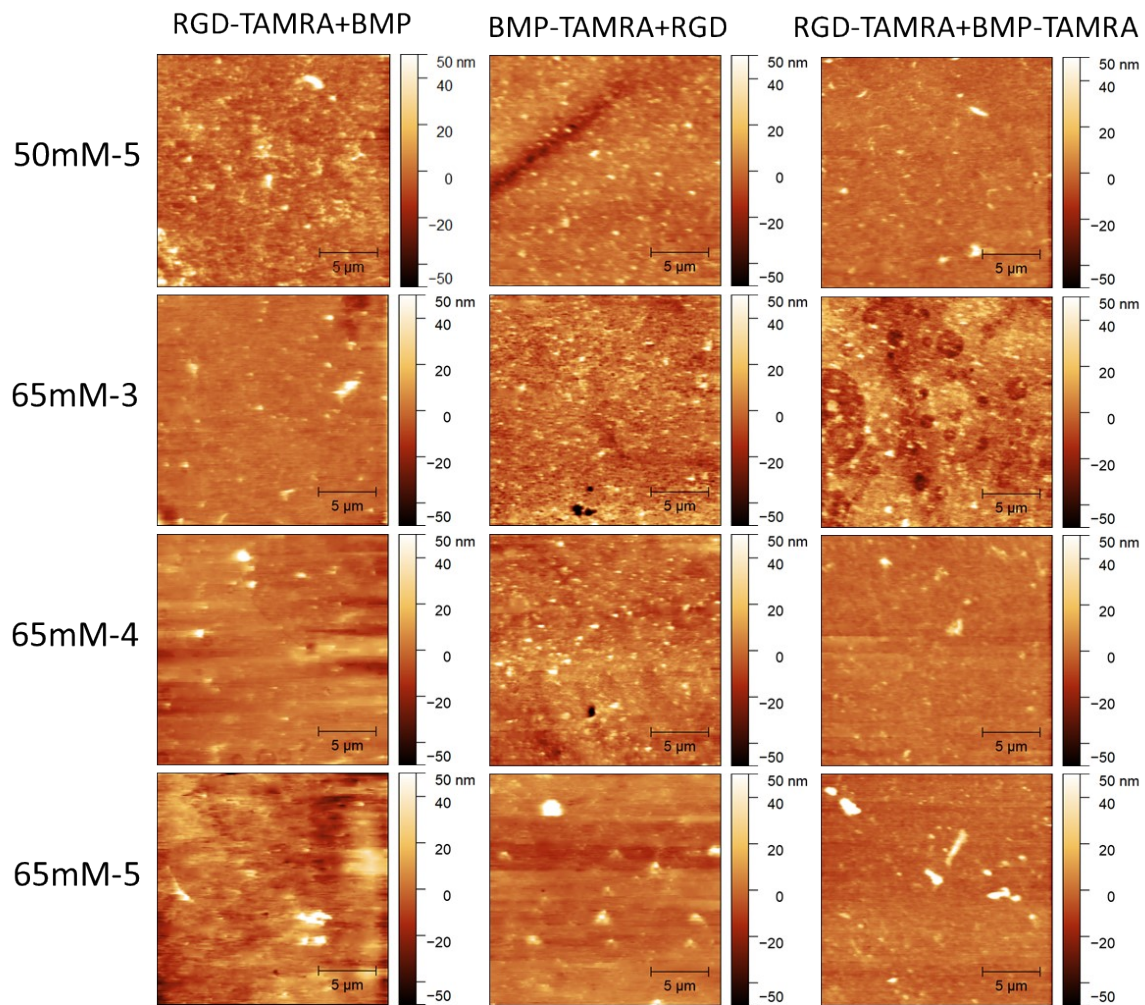


**Figure S8: surface topography (height sensor images) of DGL G5-PEG hydrogels after surface functionalization with peptides.** Three representative images, measured over 400 μm<sup>2</sup> each, are shown per condition, reporting surfaces grafted with GRGDSPC-TAMRA+BMP-2 bp (left), BMP-2-TAMRA bp + GRGDSPC (middle) and GRGDSPC-TAMRA + BMP-2-TAMRA bp (right).

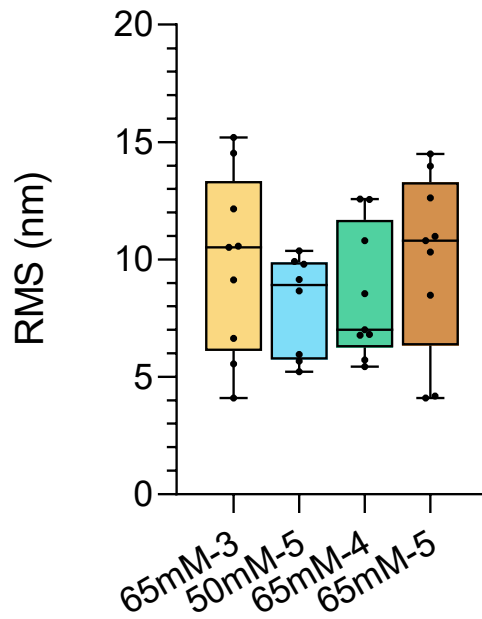
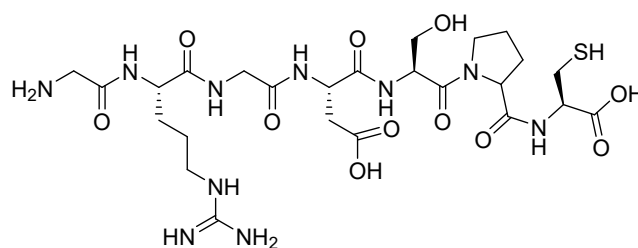
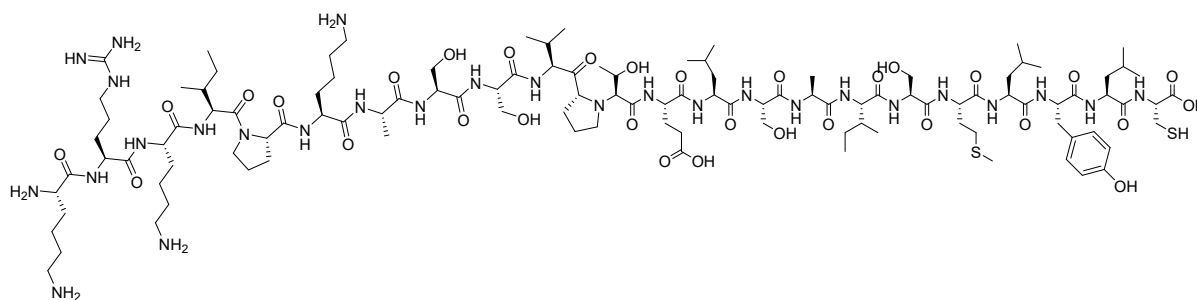


**Figure S9: root mean square roughness (RMS) of selected DGL G5-PEG hydrogel surfaces after peptide grafting to the surface.** Each point represents the averaged RMS value over a squared array of  $400 \mu\text{m}^2$  ( $20 \times 20$ ). At least three different regions were analysed per gel. N (gels) = 3, One-way ANOVA (Tukey's correction for multiple comparisons) with  $P < 0.05$  (\*),  $P < 0.01$  (\*\*),  $P < 0.001$  (\*\*\*). Not significant =  $P > 0.05$ . All statistical tests are reported at the end of the Supplementary Information.



GRGDSPC peptide (A)



KRKIPKASSVPTELSAISMLYLC peptide (BMP-2 bp, B)

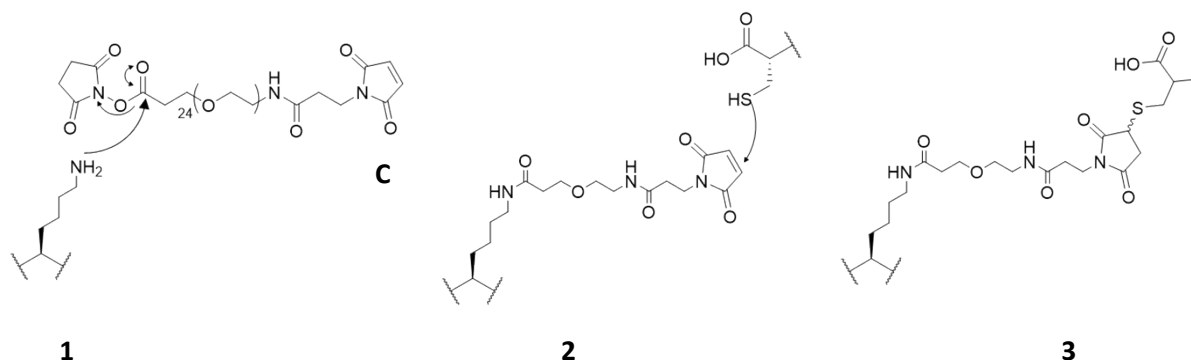
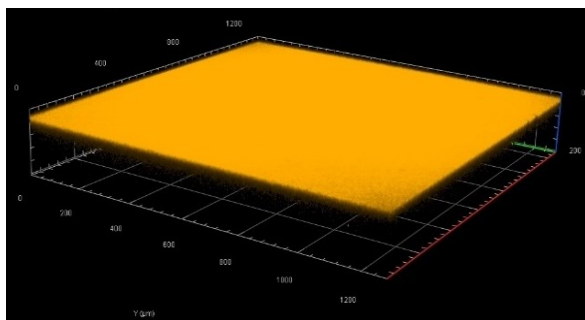


**Figure S10: surface functionalization strategy of DGL G5-PEG hydrogels after crosslinking.** Cysteine-containing peptides, the GRGDSPC (A) and BMP-2 bp (B), are covalently grafted using a maleimide-PEG-NHS spacer (C). This spacer is first reacted with the free  $\alpha$  (not shown) and  $\epsilon$ -amine groups available on DGL G5 surfaces via a nucleophilic substitution (eliminating N-hydroxysuccinimide, not shown) in 10mM phosphate buffered solution at pH 7.3 (1). Then, once hydrogel surfaces are activated by exposing maleimide units (2), the peptides are selectively conjugated at the C-ter (Cys) via a thiol-maleimide reaction in 10mM phosphate buffered solution at pH 7.3. Possibly, maleimide hydrolysis leads to ring opening but not peptide lost.

GRGDSPC-TAMRA + BMP-2 bp



BMP-TAMRA bp + GRGDSPC

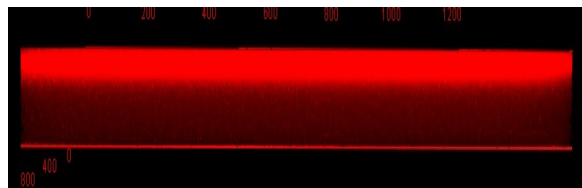
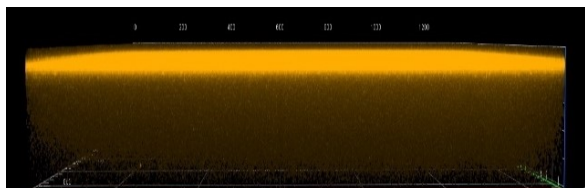
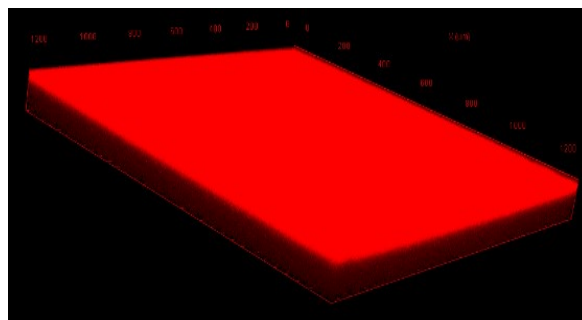


**Figure S11: 3D-reconstruction of a Z-stack obtained in confocal microscopy of 50mM-5 DGL G5-PEG hydrogels.** It shows that the highest fluorescence intensity of TAMRA-tagged peptides is present at the hydrogel's top surface layers, over a gradient of about 50 microns. Pixel intensities were adjusted to avoid oversaturation of most intense layers (10x objective, 0.45 NA).



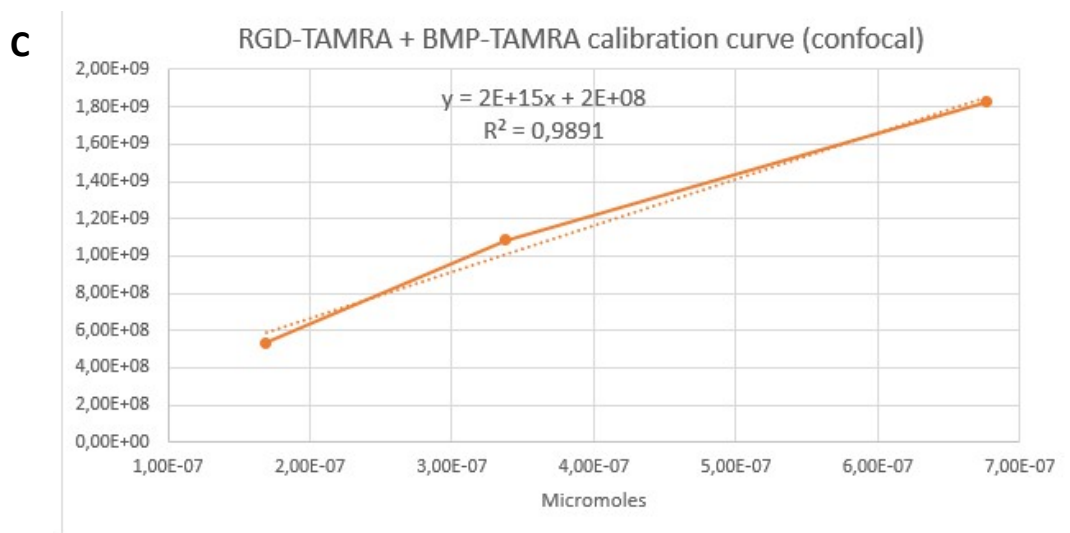
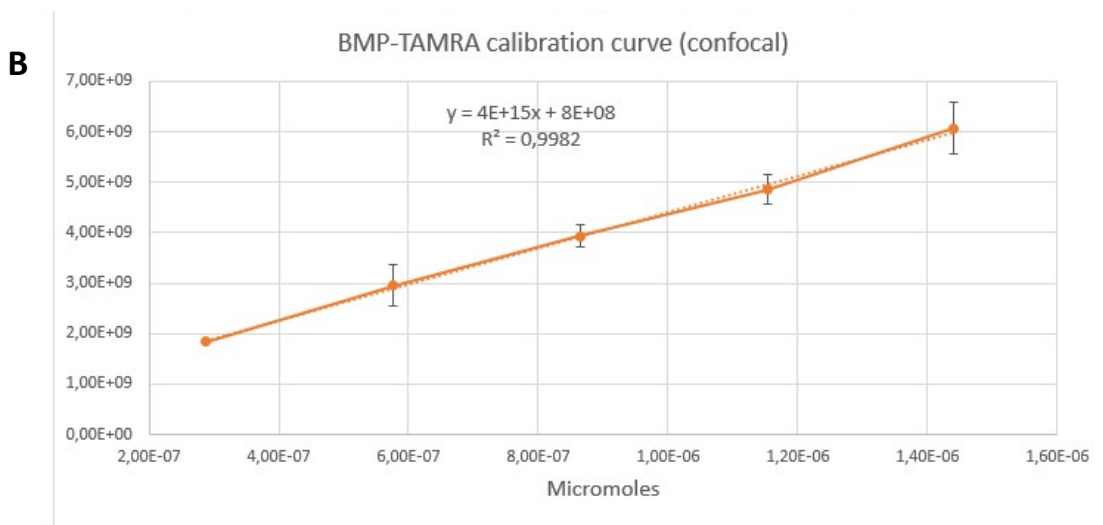
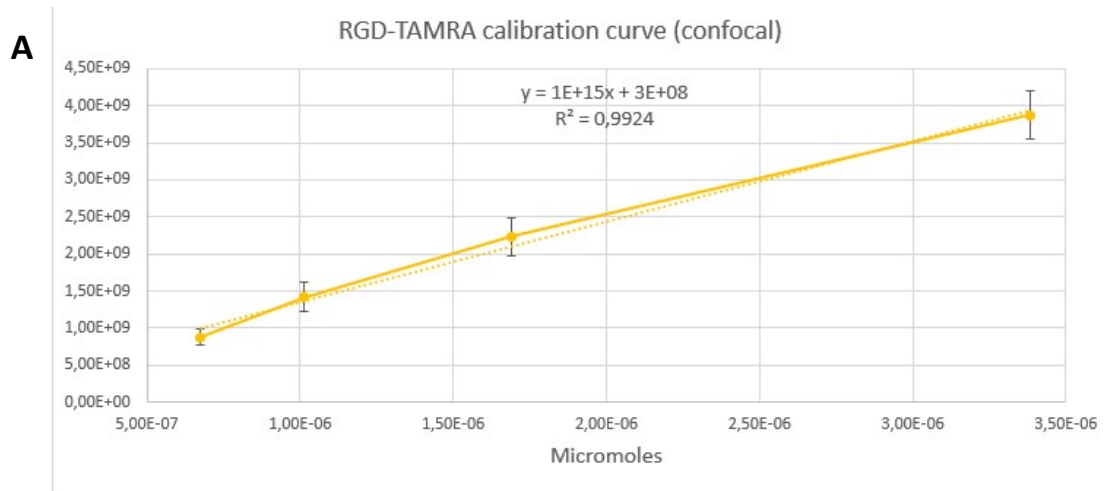


**Figure S12: calibration curves for fluorescent peptides combinations.** The curves were obtained in confocal microscopy for GRGDSPC-TAMRA peptides (yellow, **A**), BMP-2-TAMRA bp (red, **B**) and 1:1 GRGDSPC-TAMRA + BMP-2-TAMRA peptide mixtures (orange, **C**).

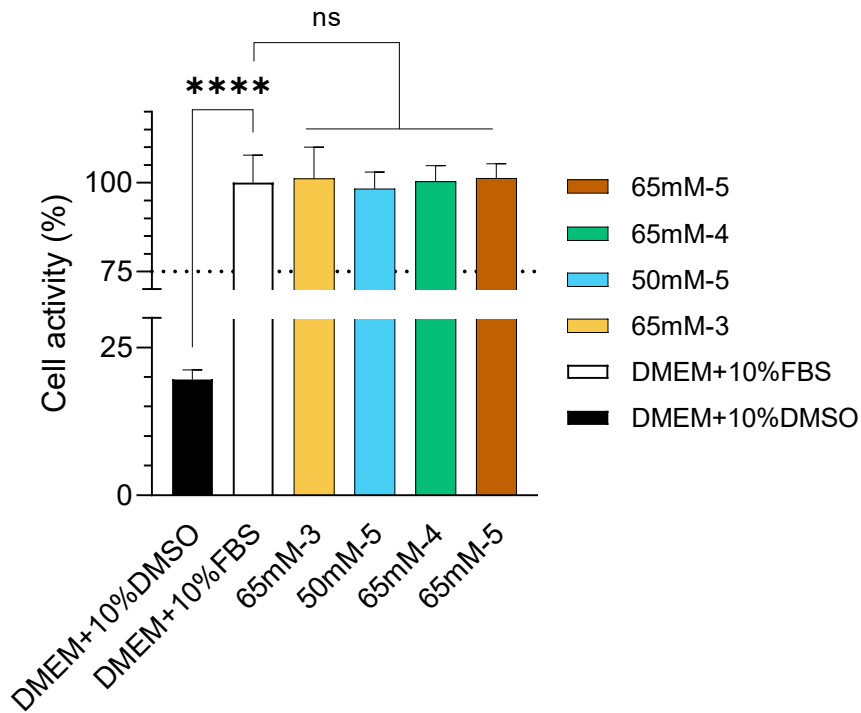


**Figure S13: undirect cytotoxicity test of unfunctionalized DGL G5-PEG hydrogels.** hMSC P5 metabolic activity (reduction potential) measured photometrically using an XTT test (O.D.<sub>490</sub> – O.D.<sub>690</sub>), normalized to cell activity in the control (DMEM+10%FBS, 100% of activity). N=6 wells per conditions, three readings per well. ONE-WAY ANOVA (uncorrected Fisher's LSD) analysis, with P<0.05 (\*), P<0.01 (\*\*), P<0.001 (\*\*\*). Not significant = P > 0.05. All statistical tests are reported All statistical tests are reported at the end of the Supplementary Information.

65mM-3

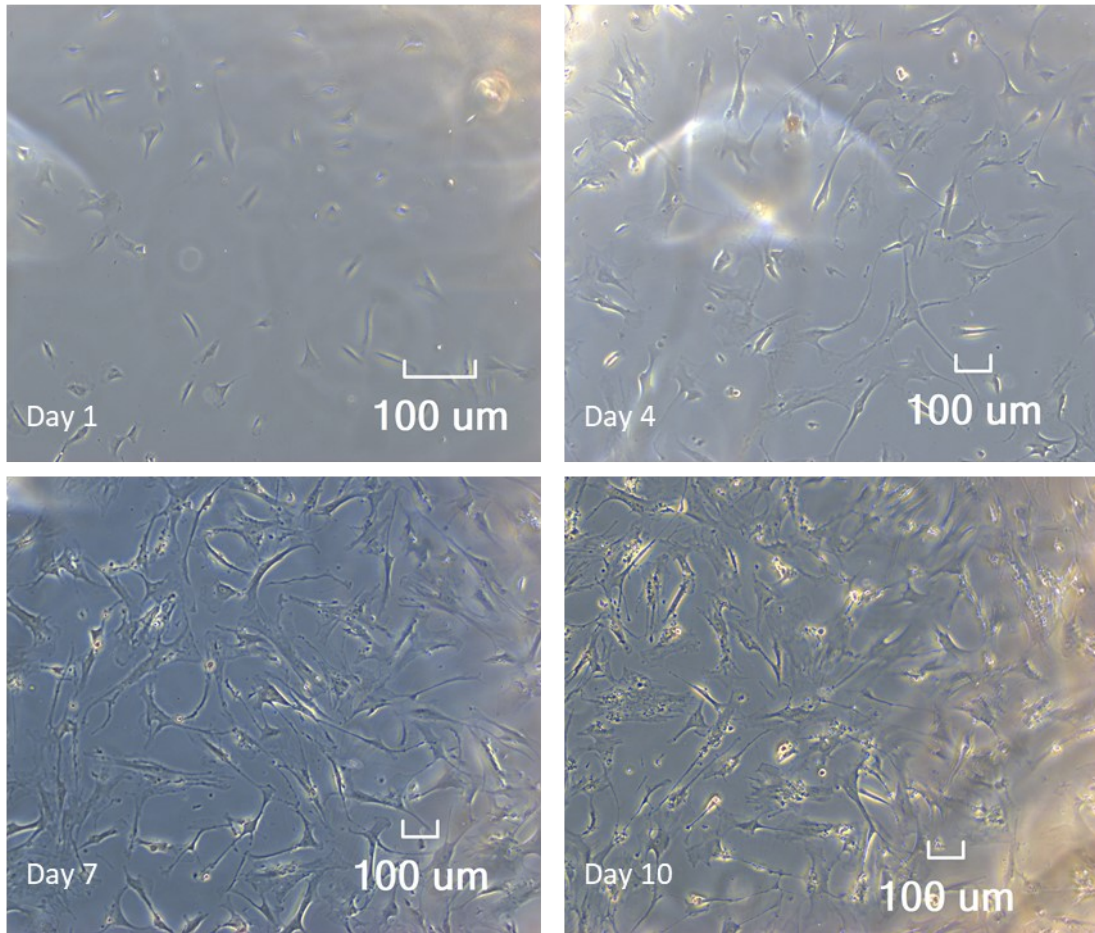


**Figure S14, A:** phase contrast images of hMSCs cultured over DGL G5-PEG hydrogels (65mM-3 condition) at different culture time points (1 day after seeding, 4 days after seeding, 7 days after seeding and 10 days after seeding) in osteogenic differentiation medium. On day 14, cells were fixed.

50mM-5

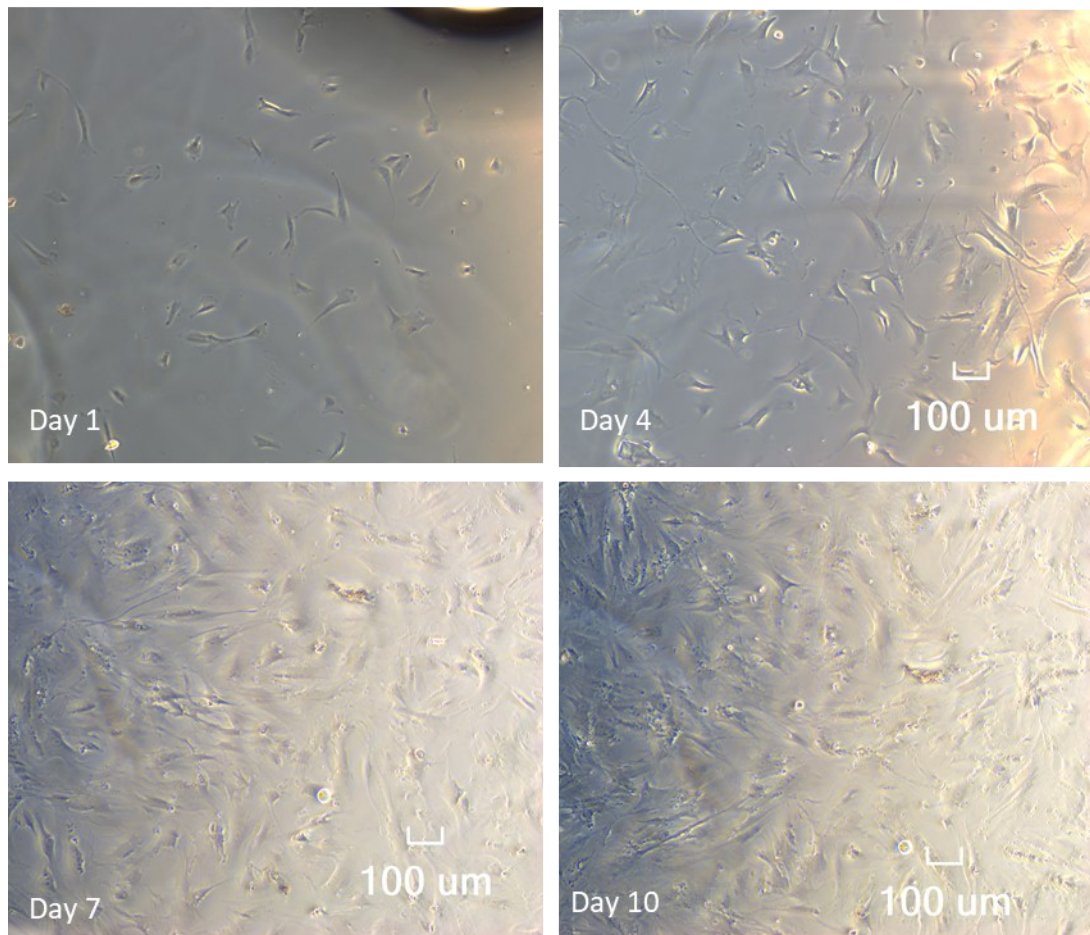


**Figure S14, B:** phase contrast images of hMSCs cultured over DGL G5-PEG hydrogels (50mM-5 condition) at different culture time points (1 day after seeding, 4 days after seeding, 7 days after seeding and 10 days after seeding) in osteogenic differentiation medium. On day 14, cells were fixed.

65mM-4

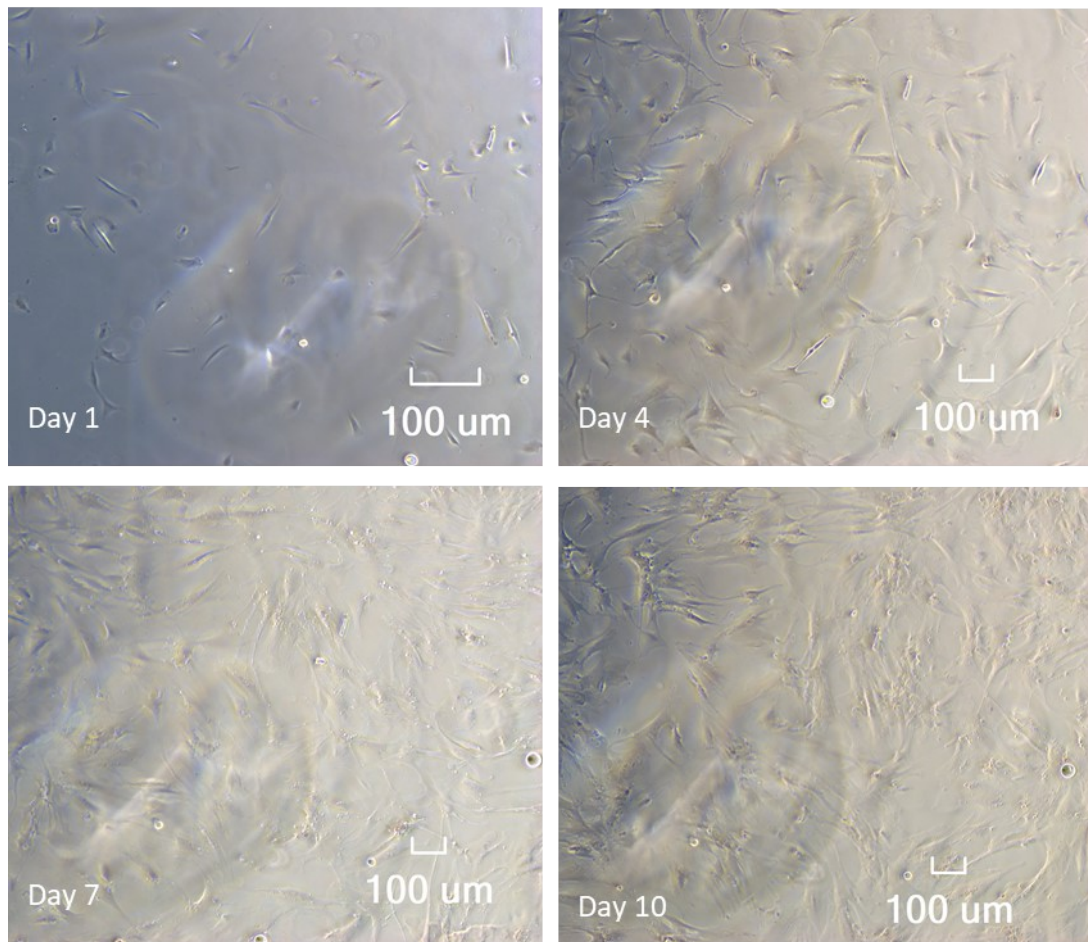


**Figure S14, C:** phase contrast images of hMSCs cultured over DGL G5-PEG hydrogels (65mM-4 condition) at different culture time points (1 day after seeding, 4 days after seeding, 7 days after seeding and 10 days after seeding) in osteogenic differentiation medium. On day 14, cells were fixed.

65mM-5

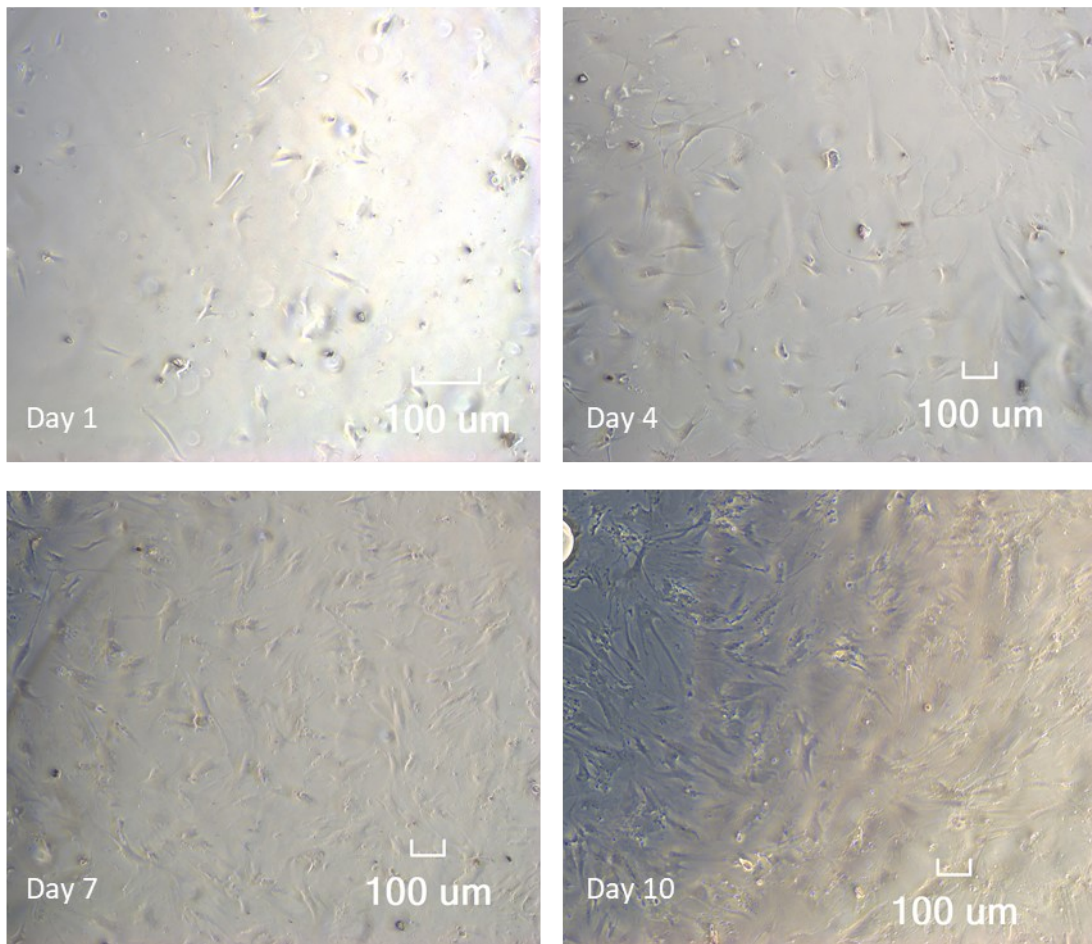


**Figure S14, D:** phase contrast images of hMSCs cultured over DGL G5-PEG hydrogels (65mM-5 condition) at different culture time points (1 day after seeding, 4 days after seeding, 7 days after seeding and 10 days after seeding) in osteogenic differentiation medium. On day 14, cells were fixed.

Glass

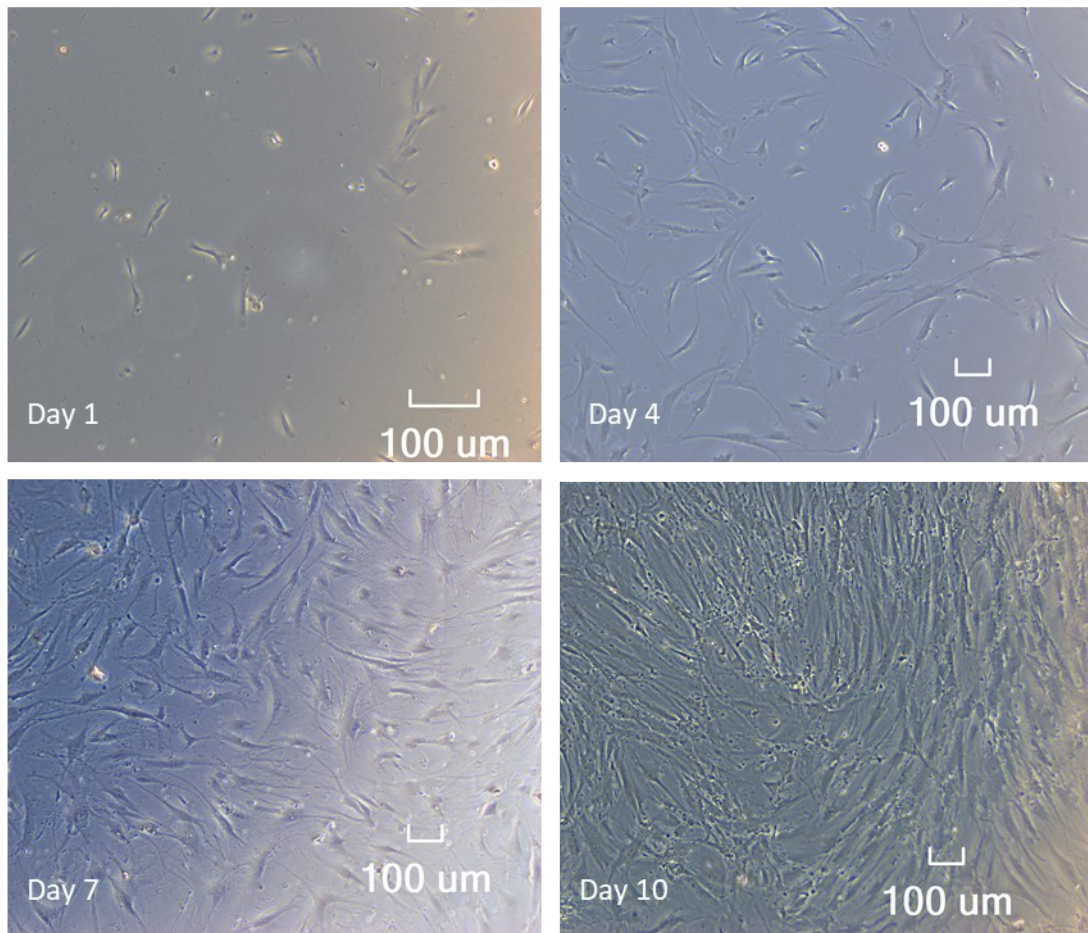


**Figure S14, E:** phase contrast images of hMSCs cultured over glass controls at different culture time points (1 day after seeding, 4 days after seeding, 7 days after seeding and 10 days after seeding) in osteogenic differentiation medium. On day 14, cells were fixed.

## Tables

Molar ratio of reactive groups in the crosslinking reaction

	[NH <sub>2</sub> /COOH] 3	[NH <sub>2</sub> /COOH] 4	[NH <sub>2</sub> /COOH] 5	[NH <sub>2</sub> /COOH] 6
[dicarboxylic-PEG] 50mM	50mM-3 [DGL-G5] 0,42 mM	50mM-4 [DGL-G5] 0,57 mM	50mM-5 [DGL-G5] 0,71 mM	50mM-6 [DGL-G5] 0,85 mM
[dicarboxylic-PEG] 65mM	65mM-3 [DGL-G5] 0,56 mM	65mM-4 [DGL-G5] 0,74 mM	65mM-5 [DGL-G5] 0,92 mM	Molar concentration of DGL-G5 in the final solution

**Table S1: formulations of DGL G5-PEG hydrogels.** The concentration of DGL G5 in the final solution (in black in the table) was calculated according to the final concentration of dicarboxylic acid-PEG (50 mM or 65 mM) and the desired excess of amines available to react per carboxylic group (NH<sub>2</sub>/COOH molar ratio, from 3 to 6).

Swelling experiments			
65mM-3	50mM-5	65mM-4	65mM-5
65mM-3	***	***	***
	50mM-5	ns	***
		65mM-4	***
			65mM-5

**Table S2: ONE-WAY ANOVA (Tuckey's correction for multiple comparisons) analysis of the fluid absorption capacity (FAC, g PBS/g dry polymer).** Calculations for equilibrium swelling experiments conducted at r.t. ONE-WAY ANOVA (with Tuckey's correction for multiple comparisons) analysis, with P<0.05 (\*), P<0.01 (\*\*), P<0.001 (\*\*\*). Not significant = P > 0.05.



Rheometry/rheometry			
65mM-3 rheometry	50mM-5 rheometry	65mM-4 rheometry	65mM-5 rheometry
65mM-3 rheometry	ns	***	***
	50mM-5 rheometry	**	***
		65mM-4 rheometry	*
			65mM-5 rheometry

Compression/compression			
65mM-3 compression	50mM-5 compression	65mM-4 compression	65mM-5 compression
65mM-3 compression	ns	***	***
	50mM-5 compression	*	***
		65mM-4 compression	*
			65mM-5 rheometry

Compression/Rheometry				
	65mM-3 rheometry	50mM-5 rheometry	65mM-4 rheometry	65mM-5 rheometry
65mM-3 compression	ns			
50mM-5 compression		ns		
65mM-4 compression			ns	
65mM-5 compression				ns

**Table S3: ONE-WAY ANOVA (Tuckey's correction for multiple comparisons) analysis of Young's modulus calculated from rheometry and compression measurements. P<0.05 (\*), P<0.01 (\*\*), P<0.001 (\*\*\*). Not significant = P > 0.05.**

65mM-3						50mM-5					
Colloidal tip		Pyramidal tip		Pyramidal tip after F.		Colloidal tip		Pyramidal tip		Pyramidal tip after F.	
m	SD	m	SD	m	SD	m	SD	m	SD	m	SD
6,41185108	0,22402177	11,925712	2,08024888	18,7863846	2,61629426	30,2851297	6,16609015	45,5132721	8,09177097	24,6066794	3,46336526
6,675798	0,39173871	9,78802953	2,18497455	20,2873649	4,98048935	29,4095809	7,53135564	44,1639	9,69122445	24,3738538	4,68857692
7,08159815	0,34665021	10,0545775	1,26432337	23,5246862	4,04336149	27,2793018	5,60822699	47,2492638	15,8506868	23,0931508	3,37334925
7,228174	0,29395381	8,60469375	1,04330724	21,3684308	3,33352409	29,2957208	6,26446249	43,477721	8,39436217	29,0347215	6,00468139
7,16657508	0,28914185	9,5891425	1,3348637	23,9489651	4,06635314	28,5021053	6,07897534	41,0479073	7,89588411	30,5696538	5,31922883
7,75669292	0,53159593	8,46368159	1,50767966	22,5003015	3,19151167	19,563962	5,85485354	38,9980661	6,44747355	30,15992	9,87699246
8,30761646	0,4434047	9,38781836	2,04052228	20,2243692	5,27057595	29,3355216	10,1127072	38,5128406	8,9687561	30,5540723	4,51220908
7,13487415	0,30626178	9,26912625	0,88707056	28,1387538	3,20673882	29,6801625	8,99608346	44,4072	12,2446637	20,2364794	3,01365724
6,89324231	0,40282683	10,2795539	1,19191723	16,6542862	3,46846763	24,7596787	8,31674616	37,5179552	7,86042722	25,7657185	3,55810055
7,12860477	0,40836316	9,58830672	0,89844102	19,836356	6,19209277	22,1541142	6,79869183	39,1349698	8,3117046	26,4282391	3,7581754
11,1231074	0,91020347	11,2858442	0,87319638	24,6847172	6,15472984	31,946934	9,01762095	42,1334422	9,25849075	49,7011953	11,2745274
16,6072646	1,23181371	12,0272878	1,74207391	29,0020422	4,7486555	25,8247321	7,72171573	40,4466813	7,3040606	43,0545615	8,99786889
19,9350431	0,57883814	11,1530042	1,27397722	26,5305692	4,75298478	29,3766474	8,15220735	39,6465188	4,94553447	40,151722	8,57246554
19,5736954	1,07716579	13,7731945	2,23448275	18,9857138	5,4112966	29,3325625	5,8863696	40,6113563	8,78088076	41,713305	9,72832418
18,1061922	0,46721598	17,2418938	1,60479585	25,2136938	5,67481667	31,7179387	7,497393	42,1556281	9,05855124	42,1730523	8,98876447
		12,1556452	1,33428099	21,3488923	4,83565528			48,0602647	10,5498745	43,7758723	6,90871558
		11,7425186	1,69307615	20,6270858	4,34555341					48,2697292	10,1256668
		11,0163416	1,5022586	23,0104692	4,62973974					48,5573587	9,84471635
		9,03439172	1,33659978	25,6040769	5,13438677					41,5999985	6,98409976
		8,87788064	1,76647697	29,1269415	4,79251062					35,6213815	5,15650395
				25,4891831	4,28299383					37,5036431	5,24032779
				25,6408234	6,0567103					37,1683127	6,4900208
										42,0049266	7,86597804

65mM-4						65mM-5					
Colloidal tip		Pyramidal tip		Pyramidal tip after F.		Colloidal tip		Pyramidal tip		Pyramidal tip after F.	
m	SD	m	SD	m	SD	m	SD	m	SD	m	SD
43,2944883	8,33799736	58,3986344	9,33694324	56,6161906	14,6369577	64,5882422	20,8221646	118,406913	34,5415209	94,4520438	22,6835238
44,987505	11,3043886	61,7977344	9,60022462	61,1607062	15,0388348	69,5554781	22,3524648	100,737898	32,3553614	98,2307525	24,0454587
52,8190869	11,0133191	60,764725	11,77928	67,7773908	12,890615	56,7853063	16,8533604	100,744469	28,1203266	101,445157	22,8038931
56,428073	14,7227498	53,5233746	6,5783633	67,6772985	12,1033675	66,6197484	22,2101219	101,539402	14,2135235	109,991738	30,2263216
47,7299175	11,1455462	57,1791469	8,19133888	86,6395662	25,5297267	66,3216031	15,3490211	101,993075	21,6282633	109,495389	20,0485596
41,718118	8,38847313	54,6038333	12,1492774	82,3380385	15,6065173	59,4777453	17,8587628	132,658847	22,5010492	113,825252	23,6414004
66,0948408	21,876907	52,9818918	15,0531276	85,13596	11,9816912	93,1225563	33,32116	130,732423	29,0388971	117,472681	24,6845025
64,5186795	18,6415442	67,5839636	29,8872813	83,6197431	14,8221598	82,83795	29,9813243	133,538122	48,0248175	114,097606	17,1153802
60,6116008	18,5394748	56,5866	17,9835774	86,03632	16,1462781	93,8361365	35,8025818	146,454905	36,6100072	113,532002	24,021818
66,8578984	20,5798081	55,4816306	29,1290599	85,06794	12,8730912	91,5876891	37,0175992	139,19515	43,0005335	128,246066	19,6978624
60,1912257	13,2038853	53,5539159	14,7359198	75,0185138	16,8233083	95,4976375	34,3984257	92,1112224	26,6637936	103,185616	30,5166957
57,4282984	16,6120989	57,3805109	10,1096068	80,4538719	16,5068645	87,0763609	23,6569687	129,462512	28,0044664	118,171487	23,2573296
58,4660361	24,2152232	48,6108281	13,9846424	78,9849781	17,4284197	88,3304406	22,304738	113,620033	25,0764695	113,497784	51,6848156
41,0076514	7,59412024	41,0868906	6,16977273	80,8545	27,271351	84,2852234	27,7218165	109,295481	28,7542025	91,9444635	30,4313151
47,8768787	11,803715	54,0002381	8,07344055	87,2484923	18,7712199	68,2699313	22,746299	102,939397	30,5827979	82,7509569	22,0077547
40,3066602	7,86686648	60,8281286	11,4960805	90,20714	24,0660088	81,42895	28,0365474	109,56618	21,3748177	154,821038	31,415581
49,8658066	11,6728929	39,5968656	5,98034283	93,4200297	21,7858396	59,8253859	13,5918116	97,1547111	20,854006	151,075443	41,2893246
50,0964223	11,3320596	49,6426453	4,36269512					99,9735266	23,8247808	139,117145	37,3525174
		48,2343734	4,16073257					92,950041	24,0939264	157,987878	36,5504816
								109,930367	25,9397111	152,866515	59,7306072
										132,53947	46,7592862
										135,899848	52,0418665
										146,6182	52,4176921
										127,802623	51,0442069
										139,441546	44,9927987
										144,485113	37,0344184

**Table S4: AFM data.** E values obtained from each hydrogel surface region, extracted from matrices of 68 (8x8) force curves measured over a squared array of 20x20 μm. E values from each surface region were averaged to obtain one mean value - so that Young's modulus of each sample (n) was represented by at least 5 mean values and each hydrogel condition by 15 mean values (n = 3). The distribution of mean values obtained with the colloidal tip is not normal, so data were statistically analysed using non-parametric tests (Kruskal-Wallis test with Dunn's correction for multiple comparisons).

Fluorescent peptide grafting of GRGDSPC-TAMRA+BMP-2-bp (RGD) mixtures vs GRGDSPC+BMP-2bp-TAMRA (BMP) mixtures											
65mM-3 RGD	50mM-5 RGD	65mM-4 RGD	65mM-5 RGD	65mM-3 BMP	50mM-5 BMP	65mM-4 BMP	65mM-5 BMP	65mM-3 RGD+BMP	50mM-5 RGD+BMP	65mM-4 RGD+BMP	65mM-5 RGD+BMP
	ns	ns	ns	ns	ns	ns	ns	***	***	***	***
65mM-3 RGD		ns	ns	ns	ns	ns	ns	***	***	***	***
	50mM-5 RGD		ns	ns	ns	ns	ns	***	***	***	***
		65mM-4 RGD		ns	ns	ns	ns	***	***	***	***
			65mM-5 RGD		ns	ns	ns	***	***	***	***
				65mM-3 BMP		ns	ns	***	***	***	***
					50mM-5 BMP		ns	***	***	***	***
						65mM-4 BMP		***	***	***	***
							65mM-5 BMP	***	***	***	***
								65mM-3 RGD+BMP	ns	ns	ns
									50mM-5 RGD+BMP	ns	ns
										65mM-4 RGD+BMP	ns
											65mM-5 RGD+BMP

**Table S5: ONE-WAY ANOVA (Tukey's correction for multiple comparisons) analysis of fluorescence intensity measurements of surface-grafted peptides reported in Fig. 4. P<0.05 (\*), P<0.01 (\*\*), P<0.001 (\*\*\*). Not significant = P > 0.05.**

Cell spreading area				
Glass control	65mM-3	50mM-5	65mM-4	65mM-5
Glass control	***	*	ns	*
	65mM-3	***	***	***
		50mM-5	ns	ns
			65mM-4	ns
				65mM-5

Aspect ratio				
Glass control	65mM-3	50mM-5	65mM-4	65mM-5
Glass control	***	ns	**	**
	65mM-3	***	ns	ns
		50mM-5	***	***
			65mM-4	ns
				65mM-5

**Table S6: Kruskal-Wallis test (with Dunn's correction for multiple comparisons) of cell spread area and aspect ratio 6h after seeding.** Data were calculated from fluorescence intensity measurements after 6h of culture in DMEM (without Red Phenol) on selected DGL G5-PEG hydrogel surfaces and in DMEM + 10%FBS for glass controls. P<0.05 (\*), P<0.01 (\*\*), P<0.001 (\*\*\*). Not significant = P > 0.05.

Cell spreading area after two weeks of culture in OM				
Glass control	65mM-3	50mM-5	65mM-4	65mM-5
Glass control	***	***	ns	ns
	65mM-3	ns	***	***
		50mM-5	***	***
			65mM-4	ns
				65mM-5

Aspect ratio after two weeks of culture in OM				
Glass control	65mM-3	50mM-5	65mM-4	65mM-5
Glass control	***	***	ns	ns
	65mM-3	ns	***	***
		50mM-5	**	*
			65mM-4	ns
				65mM-5

Cell (nuclei) counts after two weeks of culture in OM				
Glass control	65mM-3	50mM-5	65mM-4	65mM-5
Glass control	***	ns	**	ns
	65mM-3	**	ns	**
		50mM-5	ns	ns
			65mM-4	ns
				65mM-5

OPN nuclear expression after two weeks of culture in OM				
Glass control	65mM-3	50mM-5	65mM-4	65mM-5
Glass control	ns	ns	***	***
	65mM-3	ns	***	***
		50mM-5	***	***
			65mM-4	***
				65mM-5

**Table S7: Kruskal-Wallis test (with Dunn's correction for multiple comparisons) of cell spread area, aspect ratio, cell counts and osteopontin expression after two weeks of culture in OM.** Data were calculated according to fluorescence intensity measurements. P<0.05 (\*), P<0.01 (\*\*), P<0.001 (\*\*\*). Not significant = P > 0.05.